

AIM OF THE WORK

The aim of this work was to study the role of Magnetic Resonance Imaging in the evaluation of bilateral basal ganglia lesions.

PATIENTS

The study was conducted on forty patients having definite or suspicious basal ganglia lesions. All were referred to Radiodiagnosis Department Faculty of medicine, University of Alexandria with neurological and non-neurological symptoms.

After approval of the Medical Ethics Committee, an informed written consent was taken from all patients.

METHODS

All patients were subjected to:

I- Full history taking and thorough clinical examination including:-

- 1) Name, age and sex.
- 2) Neurological and non-neurological symptoms and signs including:
 - Disturbed level of consciousness, epilepsy, macrocephaly.
 - Abnormal movement: ataxia ,dystonia, chorea , rigidity
 - Psychomotor regression, mental detrition.
 - Acute respiratory distress, perinatal hypoxia, drug intake.
 - Delayed puberty, ascites, lymphadenopathy and fever

II- Imaging study:-

Brain MRI study was mainly performed on a 1.5T magnet Philips Gyroscan Intera closed configuration whole body scanner using a standard quadrature head coil, besides GE1.5T and Siemens 1.5T.

The patients' heads were positioned in a vacuum pillow to avoid head mal-rotation with the following parameters:

Patient Entry	Head First
Patient Position	Supine
Coil Configuration	Head coil

- All patients were subjected to the following MRI protocols:-

A) Conventional MRI:

1. Axial T1 weighted image utilizing the following parameters:
 - A repetition time (TR) of 400-500 m sec, an echo time (TE) of 15 m sec, TI of 2000 m sec, a slice thickness of 5 mm and FOV= 230 mm.
2. Axial T2 weighted image utilizing the following parameters:
 - A repetition time (TR) of 4000 m sec, an echo time (TE) of 100 m sec, a slice thickness of 5 mm, FOV= 230 mm.
3. Axial FLAIR utilizing the following parameters:
 - A repetition time (TR) of 6000 m sec, an echo time (TE) of 120 m sec, TI of 2000 m sec, a slice thickness of 5 mm and FOV= 230 mm.
4. Axial DWI utilizing the following parameters:
 - A repetition time (TR) of 1000 m sec, an echo time (TE) of 100 m sec, TI of 2000 m sec, a slice thickness of 5 mm and FOV= 230 mm.

B) Advanced MRI (done whenever needed).

1. Axial SWI utilizing the following parameters:

- A repetition time (TR) of 500 m sec, an echo time (TE) of 15 m sec, TI of 2000 m sec, a slice thickness of 5 mm and FOV= 230 mm.

2. MRS multi-voxel was done by using point resolved spectroscopy (PRESS) sequences. The volume of interest (VOI) size and position were determined by examining the scout MR vipers in the three dimensions (sagittal, coronal and axial planes), with the aim to include the largest portion of the basal ganglia lesions, peri-lesional area together with normally appearing brain within the region of interest as much as we can and to exclude subcutaneous fat and regions with large variations in magnetic susceptibility (i.e. the sinuses and bony calvarium). Multi-voxel spectroscopy was performed using intermediate echo time of 135 m sec (TR 1500 m sec, FOV 160 mm).

Patients who needed sedation were given the sedative dose of thiopental sodium 3mg/kg.

C) Image analysis:

- Identify the lesion.
- Identify being unilateral or bilateral.
- Identify the affected basal ganglia nuclei.
- The symmetry of the nuclear affection.
- Identifying the signal abnormalities.
- Look for the presence or absence of thalamic affection and other associated radiological abnormalities of the brain.
- Correlation with the laboratory and clinical data.

RESULTS

This study included 40 patients mainly presented with neurological manifestations and referred to the radiological department at Alexandria main university hospital (22 males and 18 females.) Their age ranged from 7 days to 69 years. Table (4).

Table (4): Distribution of patients according to different age groups:

Age Categories	Number	Percentage
<10 years	20	50%
10-20 years	6	15%
20-30 years	1	2.5%
30-40 years	1	2.5%
40-50 years	5	12.5%
50-60 years	5	12.5%
60+ years	2	5%
Total	40	100%

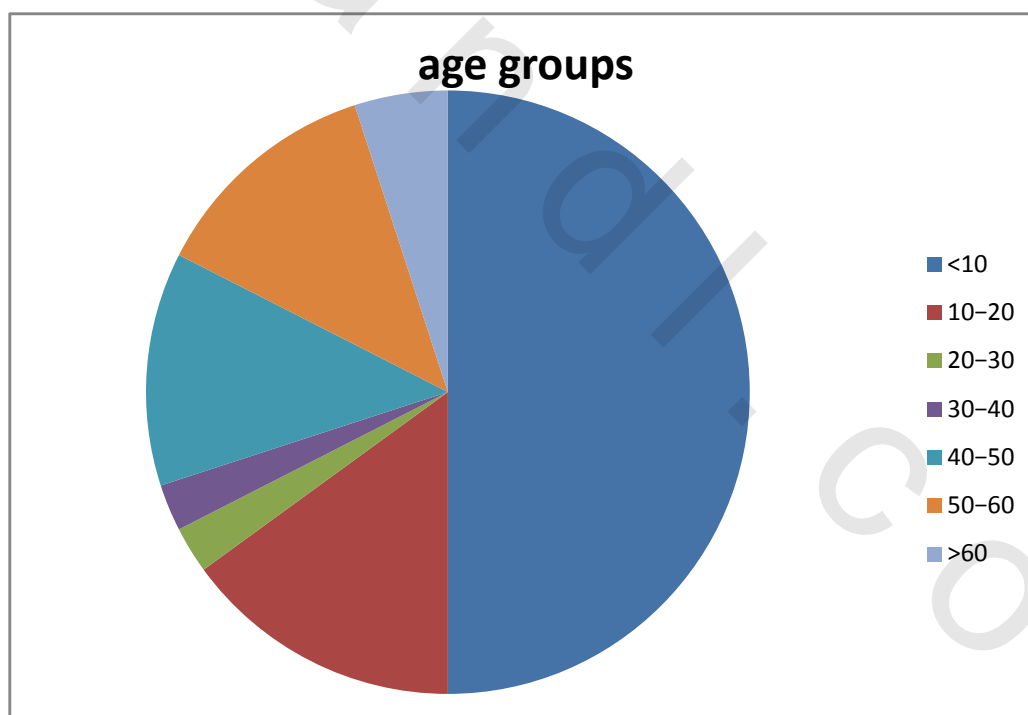


Fig 31: Distribution of patients according to different age groups

All patients considered the examination acceptable, and no discomfort or complications were found by care takers.

They were distributed according to the gender, with male sex predominance as males representing 55%, females representing 45%.Fig. (32).

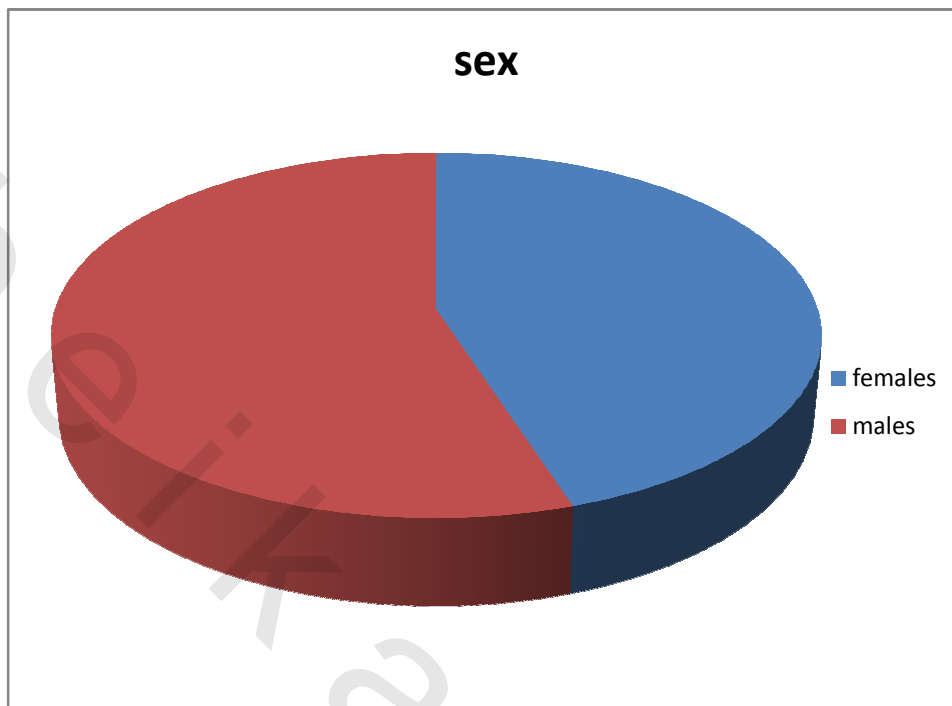


Fig. 32: Distribution of patients according to the gender.

Table (5): The final suggested diagnosis reached by cMRI and MRS:

No of patients	Final diagnosis
1	Hallervorden-Spatz syndrome
1	Huntington disease.
7	Leigh disease.
5	Icteric encephalopathy.
5	Hepatic failure.
1	Endocrine abnormality (hypopituitarism).
1	Extra pontine osmotic myelinolysis.
2	Glutaric acidemia type I.
6	Hypoxic ischemic encephalopathy.
1	Global ischemia.
1	Ischemia.
1	Toxoplasmosis.
3	Toxic (CO poisoning ,calmepam,unknown.).
2	Virchow Robin spaces.
1	Metastasis.
1	Lymphoma.
1	venous thrombosis.

The studied patients have been classified into two groups; pediatric age group and adult age group. The pediatric age group accounted for 60% of the examined patients while the adult age group represented 40% of the examined patients. Table (6).

Table (6). Distribution of patients according to the age groups.

Age group	patients	Number	Percentage
pediatric	HIE	5	12.5%
	Venous thrombosis.	1	2.5%
	Leigh disease.	7	17.5%
	Extra pontine osmotic myelinolysis.	1	2.5%
	Glutaric acidemia type I.	2	5.0%
	Endocrine abnormality (hypo pituitarism.)	1	2.5%
	Icteric encephalopathy.	5	12.5%
	Huntington disease.	1	2.5%
	Hallervorden-spatz syndrome.	1	2.5%
Total	Pediatric	24	60%
Adult	HIE.	1	2.5%
	Global ischemia.	1	2.5%
	Ischemia.	1	2.5%
	Hepatic failure.	5	12.5%
	Vichow Robin spaces.	2	5.0%
	Toxoplasmosis.	1	2.5%
	Toxic.	3	7.5%
	Lymphoma.	1	2.5%
	Metastasis.	1	2.5%
Total	Adult.	16	40.00%
Total	Adult +pediatric.	40	100%

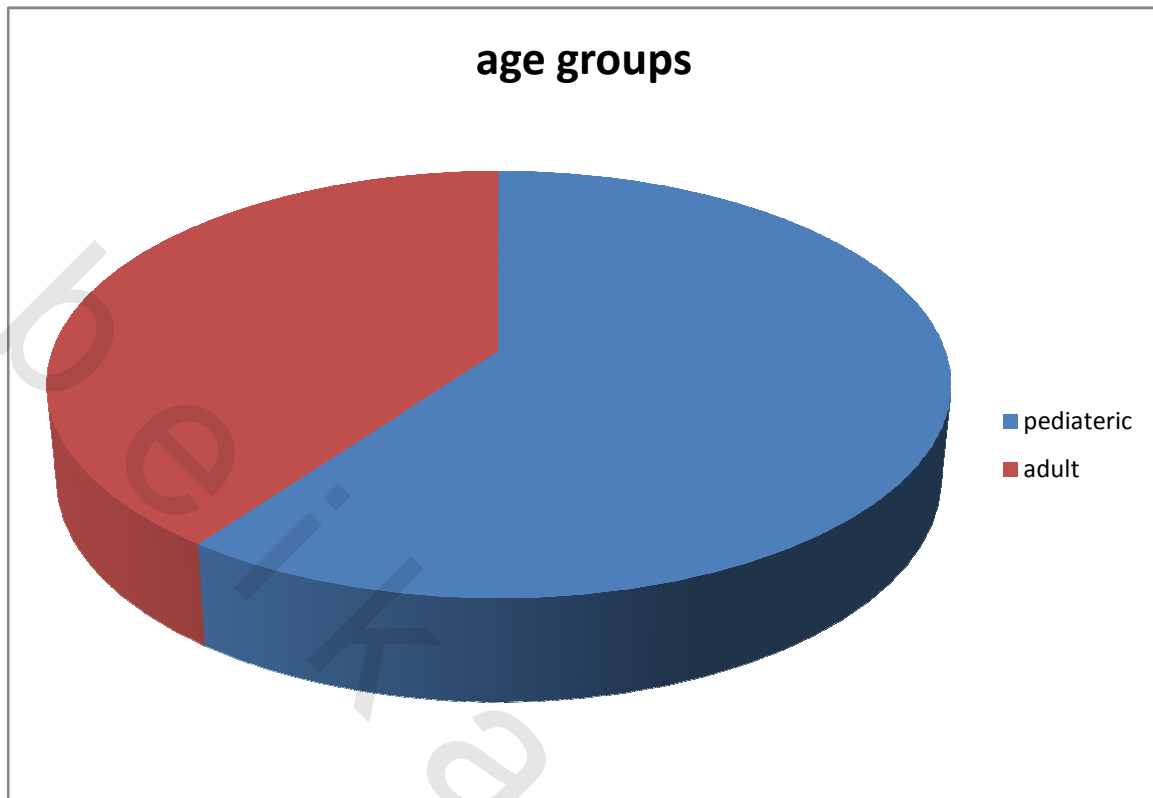


Fig. 33: Distribution of patients according to the age groups.

The studied patients have been classified according to the clinical presentation; acute or chronic presentation, acute presentation defined as condition of rapid onset and/or a short course, while chronic presentation defined as illness lasting longer than three to six months. Acute presentation was the commonest and accounted about 65% followed by the chronic presentation which accounted about 35%. Table (7).

Table (7): Distribution of the patients according to the onset of the clinical presentation regardless the final diagnosis of the basal ganglia lesions.

Presentation	patients	Number	Percentage
Acute	Ischemia.	1	2.5%
	HIE.	6	15%
	global ischemia	1	2.5%
	Venous thrombosis.	1	2.5%
	Extra pontine osmotic myelinolysis.	1	2.5%
	Leigh disease.	7	17.5%
	Toxoplasma infection.	1	2.5%
	Toxic.	3	7.5%
	Icteric encephalopathy.	5	12.5%
Acute	Total.	26	65%
Chronic	Hepatic failure.	5	12.5%
	Endocrine abnormality (hypopituitarism.)	1	2.5%
	Hallervorden-Spatz syndrome	1	2.5%
	Huntington disease.	1	2.5%
	Virchow Robin spaces.	2	5%
	Glutaric acidemia type I	2	5%
	Lymphoma.	1	2.5%
	Metastasis.	1	2.5%
Chronic	Total.	14	35%
Acute+Chronic	Total.	40	100%

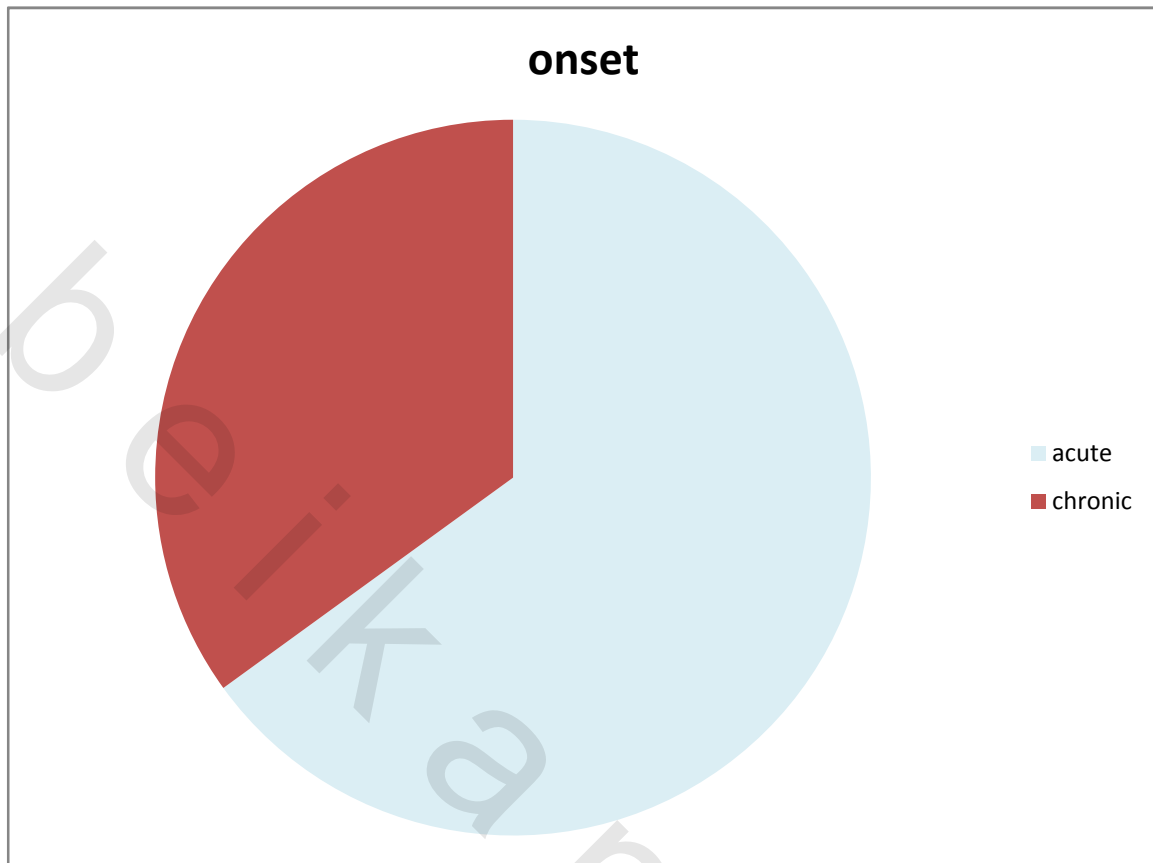


Fig. 34: Distribution of the patients according to the onset of the clinical presentation regardless the final diagnosis.

The studied patients have neurological and non-neurological manifestations; the neurological manifestations were: epilepsy, dystonia, ataxia, psycho-motor regression, mental deterioration, disturbed level of consciousness, chorea, nystagmus, rigidity, dysarthria, tremors, headache, macro-cephaly, hemiplegia and decreased visual acuity while the non-neurological manifestations were acute respiratory distress, drug intake, fever, ascites, delayed puberty, perinatal hypoxia, and lymphadenopathy. Table (8).

Table (8): Distribution of patients according to the different clinical presentations.

Clinical presentation	Number	Percentage
Neurological		
Disturbed level of consciousness.	4	10%
Epilepsy.	12	30%
Headache.	4	10%
Macrocephaly.	2	5%
Ataxia.	7	17.5%
Dystonia.	10	25%
Dysarthria.	2	5%
Mental deterioration.	4	10%
Psychomotor regression.	8	20%
Rigidity.	2	5%
Chorea.	3	7.5%
Nystagmus.	6	15%
Tremors.	5	12.5%
Hemiplegia.	1	2.5%
Hypotonia.	5	12.5%
Non neurological		
Acute respiratory distress.	3	7.5%
Delayed puberty.	1	2.5%
Drug intake.	3	7.5%
Perinatal asphyxia.	4	10%
Ascites.	5	12.5%
Jaundice.	10	25%
Lymphadenopathy.	1	2.5%
Fever.	1	2.5%
High pitched cry.	5	12.5%

Most of the patients presented with more than one symptom (neurological and non-neurological).

The studied patients were classified according to the pathological categories into seven categories; Toxic, neoplastic, metabolic, degenerative, vascular, dilated perivascular space and inflammatory conditions. In these categories, metabolic category had the highest frequencies representing 70 % followed by toxic representing 7.5% then neoplastic, vascular, degenerative and dilated perivascular space representing 5% for each one and lastly the inflammatory category represented 2.5%.Table (9).

Table (9): Distribution of patients according to different Pathological categories:

Pathological Categories	Number	Percentage
Metabolic.	28	70%
Toxic.	3	7.5%
Vascular.	2	5%
Neoplastic.	2	5%
Degenerative.	2	5%
Inflammatory.	1	2.5%
Dilated perivascular spaces (VRS.)	2	5%
Total	40	100%

The studied patients were classified according to the different pathological category and their different sub-groups. Table (10).

Table (10): Distribution of patients according to the different pathological category and their sub-groups:

Pathological category	Sub -group	No.	Percentage
Metabolic.	Leigh disease.	7	17.5%
	HIE.	6	15%
	Global ischemia.	1	2.5%
	Hepatic failure.	5	12.5%
	Glutaric acidemia type I.	2	5%
	Endocrine abnormality hypopituitarism.	1	2.5%
	Icteric encephalopathy.	5	12.5%
	Extra pontine osmotic myelinolysis.	1	2.5%
Vascular	Ischemia.	1	2.5%
	Venous thrombosis.	1	2.5%
Inflammatory	Toxoplasmosis.	1	2.5%
Dilated perivascular spaces.	Virchow Robin spaces.	2	5%
Degenerative	Hallervorden -Spatz syndrome.	1	2.5%
	Huntington disease.	1	2.5%
Toxic	CO poisoning.	1	2.5%
	Cal mipam poisoning.	1	2.5%
	Unknown toxin.	1	2.5%
Neoplastic.	Lymphoma.	1	2.5%
	Metastasis.	1	2.5%
Total		40	100%

The studied patients were classified according to the symmetry of nuclear affection whether bilateral symmetrical or bilateral asymmetrical affection of the basal ganglia. The most common was the symmetrical affection of the basal ganglia nuclei representing 85% with predominance of the metabolic category which represents 70%, while asymmetric affection of the basal ganglia nuclei representing 15%. Table (11, 12).

Table (11): Distribution of patients presented by asymmetrical basal ganglia nuclei affection.

Asymmetrical nuclear affection		No	Percentage
Pathological category	Sub-group		
Vascular	Ischemia.	1	2.5%
Inflammatory	Toxoplasmosis	1	2.5%
Dilated perivascular spaces	Dilated Virchow Robin spaces (VRS.)	2	5%
Neoplastic	Lymphoma.	1	2.5%
	Metastasis.	1	2.5%
Total		6	15%

Table (12): Distribution of patients presented by symmetrical basal ganglia nuclei affection.

Symmetrical nuclear affection		No	Percentage
Pathological category	Sub-group		
Metabolic	Hypoxic ischemic encephalopathy.	6	15%
	Global ischemia.	1	2.5%
	Leigh disease.	7	17.5%
	Icteric encephalopathy.	5	12.5%
	Hepatic failure.	5	12.5%
	Glutaric acidemia type I	2	5%
	Extra pontine osmotic myelinolysis.	1	2.5%
	Endocrinal abnormality (hypo pituitarism)	1	2.5%
Metabolic	Total	28	70%
Toxic	Toxic.	3	7.5%
vascular	Venous thrombosis.	1	2.5%
Degenerative	Huntington disease.	1	2.5%
	Hallervorden-spatz syndrome.	1	2.5%
Symmetrical	Total	34	85%

The studied patients were classified according to MRI and MRS diagnosis matching with the clinico-laboratory diagnosis &/or the histo-pathological data.95% of the patients their cMRI and MRS diagnosis were matching with the clinic-laboratory data and 5 % matching with the histo-pathological examination. Table (13).

(Two patients have stereotactic biopsy and histo-pathologically diagnosed as neoplastic lesions lymphoma and metastasis.).

Table (13): Distribution of patients according to: cMRI and MRS diagnosis matching with the clinico-laboratory and histo-pathological data.

MRI ,MRS diagnosis matching with	No	Percentage
Clinic-laboratory diagnosis.	38	95%
Histo-pathological diagnosis	2	5%
Total	40	100%

The studied patients were classified according to the different laboratory findings in the thirty eight patients with relation to their pathological category and final diagnosis.Distribution of the patients according to the different laboratory and histo-pathological findings in relation to their pathological category and final diagnosis. Table (14).

Table (14): Distribution of the patients according to the different laboratory and histo-pathological findings in relation to their pathological category and final diagnosis.

Pathological category	Diagnosis.	Lab findings	No of cases.
Metabolic	Leigh disease	Elevated serum lactate level, lactate /pyruvate ratio.	7
	HIE	Metabolic acidosis.	6
	Global ischemia	Metabolic acidosis.	1
	Hepatic failure.	Elevated serum ammonia. Elevated liver enzyme. Hypo protienemia. Anemia.	5
	Glutaric acidemia I	Increased urine organic acid.	2
	Endocrine abnormality hypopituitarism.	Hypocalcemia. Decreased level of testosterone and parathyroid hormone.	1
	Icteric encephalopathy.	Hyper billirubinemia	5
	Extra pontine osmotic myelinolysis.	Hyponatremia. Increase osmolality.	1
Vascular	Ischemia	Hypercholesterolemia.	1
	Venous thrombosis.	Metabolic acidosis.	1
Dilated perivascular spaces	Virchow- Robin spaces.	No recommended laboratory test.	2
Inflammatory.	Toxoplasmosis.	Anti-toxoplasma IgG.	1
Degenerative	Hallervorden -Spatz syndrome	Normal serum Fe.	1
	Huntington disease.	No recommended laboratory test.	1
Toxic	CO poisoning	Elevated carboxy haemoglobin level. Metabolic acidosis.	1
	Calmepam poisoning.	Metabolic acidosis.	1
	Unknown toxin.	Metabolic acidosis.	1
Neoplastic.	Lymphoma.	Histo-pathological examination revealed lymphoma.	1
	Metastasis.	Histo-pathological examination revealed metastatic deposit	1

Table (15): Represents the imaging findings of the cases by the c MRI.

patient	Nuclei affected	T1	T2	FLAIR	Enhancement	Associated related abnormality
Adult HIE.	Caudate putamen	iso	↑	↑	No.	No mass effect associated.
Pediatric HIE	Caudate putamen	↓	↑	↑	No.	Mass effect; indenting the frontal horn
Sub-acute profound HIE	Whole basal ganglia.	↑	↓	↑	No.	Affection of perirolandic cortex
Acute profound HIE	Whole basal ganglia.	↑	↑	↑	No.	Posterior limb of the internal capsule, perirolandic cortex and ventrolateral aspect of thalamus.
Prolonged profound HIE.	Whole basal ganglia.	↑	↓	↓	No.	Thalamus, cortex and white matter.
Preterm HIE.	Whole basal ganglia	iso	↑	↑	No.	Thalamic affection Encephalomalacic changes of the periventricular and deep white matter. sub cortical gliosis
Ischemia.	Caudate putamen	↓	↑	↓	No.	Thalamic hemorrhage.
Global ischemia.	Caudate putamen	↓	↑	↑	No.	Diffuse gyral and hippocampal swelling.
Leigh disease:						
▪ 1 Case	Caudate lentiform	iso	↑	↑	No.	Cerebral peduncle.
▪ 2 Cases	Caudate lentiform	iso	↑	↑	No.	
▪ 1 Cases	Globus pallidus	↓	↑	↓	No.	
▪ 2 Cases	Caudate lentiform	↓	↑	↑	No.	Cerebral peduncle and periaqueductal.
▪ 1 Case	Caudate putamen	↓	↑	Heterogeneous.	No.	Frontal cortex involvement.
Hepatic disease:						
▪ 2 Cases	Globus pallidus	↑	iso	iso	No.	Periventricular and deep white matter and pituitary gland.
▪ 3 Cases	Globus pallidus	↑	iso	iso	No.	

Table (15): Represents the imaging finding of the cases by the cMRI. Cont.

patient	Nuclei affected	T1	T2	FLAIR	enhancement	Associated related abnormality
Kernicterus: ▪ 5 cases	Globus pallidus.	↑	iso	iso	No.	↑T1 Sub thalamic nuclei
Glutaric acidemia I	Caudate lentiform	iso	↑	↑	No.	Wide operculum, temporal hypoplasia.
Glutaric acidemia I	Caudate lentiform	↓	↑	↑	No.	Wide operculum, temporal hypoplasia, ↑T2 signal white matter.
Hypo pituitarism	GP mainly	↑	iso	↑	No.	Small pituitary gland.
Extra Pontine osmotic myelinolysis.	lentiform	iso	↑	↑	No.	Parieto –occipital cortex.
Hallervorden-Spatz syndrome.	Globus pallidus	↓	↓	↓	No.	
Huntington.	Caudate putamen	↓	↑	↓	No.	Dilated frontal horn.
Toxoplasma.	Caudate putamen	↓	↑	↑	Irregular ring enhancement	Scattered lesion in the brain and cerebellum.
V.R.S.: ▪ 2 cases	Caudate putamen	↓	↑	↓	No.	
Venous thrombosis	Basal ganglia	↑	↑	↑	No.	Thalamic affection.
Co toxin	Gp mainly	↑	↑	↑	No.	White matter involvement.
Calmebam over dose.	Caudate putamen	↓	↑	↑	No.	Hemorrhagic frontal lobe
Unknown Toxin	Caudate putamen	↓	↑	↑	No.	
Lymphoma.	Body of caudate.	↓	↓	↓	Mild homogeneous enhancement.	Periventricular white matter.
Metastasis.	basal ganglia	↓	↑	↑	Heterogeneous enhancement.	Scattered within the cerebral hemisphere.

Table (16): Represents the imaging findings of the patients by the advanced MRI techniques.

Patient	Diffusion.	SWI	MRS
Adult HIE.	Restricted.	-	Decreased NAA/Cr & NAA/Cho ratios. Detectable lactate peak.
Pediatric HIE.	Restricted.	-	
Sub-acute profound HIE.	Not.	-	
Acute profound HIE	Restricted.	-	
Prolonged profound HIE.	Restricted.	-	
Preterm HIE.	Restricted.	-	
Old lacunar infarct/ischemia.	Not.	-	
Global ischemia	Restricted.	-	
Leigh disease			Prominent lactate peak in lesional areas with mild increase in Cho/cr ratio. Detectable lactate peak even in normal appearing white matter with mild increase in Cho/NAA ratio.
▪ 6 Cases	Restricted.	-	
▪ 1 Case	Not	-	
Hepatic failure ▪ 5 Cases	Not.	-	
Kernicterus ▪ 5 Cases	Restricted.	-	
Glutaric acidemia type I. ▪ 2 Cases	Not	-	
V.R.S. ▪ 2 Cases	Not.	-	
Hypo pituitarism	Not	Blooming.	
Extra pontine osmotic myelinolysis.	Restricted	-	
Hallervorden-Spatz syndrome.	Black out.	Blooming.	Decreased NAA/cr ratio.
Huntington.	Not.	-	
Toxoplasma.	Not.	Blooming.	Prominent lipid peak and dominant in most of the voxels while decreased Cho,cr and NAA peaks.
Venous thrombosis.	Restricted.	Blooming.	
Co toxin.	Restricted.	Blooming.	
Calmepam over dose.	Not.	Blooming.	
Unknown toxin.	Not.	-	
Lymphoma.	Restricted.	-	Increased Cho/cr ratio up to 10 (depleted cr). Increased Cho/NAA ratio up to 4&dominant in many voxels.
Metastasis.	Minor foci of restriction mainly marginal	No.	Increased Cho/cr ratio up to 3. Increased Cho/NAA ratio upto2.5. Detectable lactate peak.

The studied patients were also classified according to the associated radiological abnormality associating the basal ganglia lesions into findings related to the same pathology or non-related findings and others have no associated MRI findings at all. Table (17, 18 and 19).

Table 17: Distribution of patients according to the associated MRI findings with the basal ganglia lesions related to the same pathology:

Disease	No of cases	Related associations.
Huntington disease.	1	Widen frontal horn.
Leigh disease.	1	Affection of the cerebral peduncle bilaterally.
Leigh disease.	2	Affection of the cerebral peduncle bilaterally & periaqueductal.
Leigh disease.	1	Affection of the frontal cerebral cortex.
Hepatic failure.	2	Affection of DWM, PVWM& hyperintense signal of pituitary.
Extra pontine osmotic myelinolysis.	1	Hyperintense signal of the cortex.
CO poisoning.	1	Affection of the white matter.
Old lacunar infarct/Ischemia.	1	Thalamic hemorrhage.
Preterm HIE.	1	Deep and periventricular WM encephalomalacic changes, subcortical gliosis, thalamic affection & atrophic changes of the brain and the cerebellar vermis.
Global ischemia.	1	Gyral /hippocampal swelling.
Sub-acute profound term HIE.	1	Affection of the posterior limb of the internal capsule, perirolandic cortex & Temporal WM edema.
Acute Profound HIE.	1	Post limb internal capsule, ventro-lateral thalamus & Perirolandic cortex.
Prolonged Profound HIE.	1	Thalamic affection, encephalomalacic changes of the cortex ,sub cortex WM and PVWM of both cerebral hemispheres.
Pediatric HIE.	1	Mass effect on lateral ventricle.
Hormonal abnormality (hypopituitarism.)	1	Decreased height of the pituitary gland
Glutaric acidemia type I	1	Dilated Sylvain fissure (wide opercular). Temporal hypoplasia Increased signal of DWM
Glutaric acidemia type I	1	Dilated Sylvain fissure (wide opercular). Temporal hypoplasia.
Toxoplasmosis.	1	Affection of thalamus, cerebellum& GWMJ.
Calmebam toxicity	1	Frontal lobe hemorrhage.
Lymphoma.	1	Mass effect, edema & periventricular lesions.
Metastasis.	1	Mass effect, edema & scattered lesions.
Venous thrombosis.	1	Thalamic hemorrhage.
Hallervorden-Spatz	1	Cerebellar atrophy.
Kernicterus.	5	Sub thalamic nucleus affection.

Table 18: Distribution of patients according to the associated MRI findings with the basal ganglia lesions unrelated to the same pathology:

patient	No of cases.	Not related pathology
Leigh disease.	1	Cavum septum pellucidum. Atrophic brain changes.
Leigh disease.	1	Cerebellar increased T2 signal.
Huntington disease.	1	Post encephalitic changes.

Table 19: Distribution of patients according to the basal ganglia lesions with no associated MRI findings:

No associations	No of cases.
Adult HIE.	1
Leigh disease.	1
Hepatic failure.	3
Unknown toxin.	1
Virchow- Robin spaces.	2

patient 1: 5 years old female presented with chronic illness in the form of sustained involuntary muscle contractions (dystonia) with oro-mandibular involvement, dysarthria, mental deterioration and ataxia, there was no history of fever, jaundice or seizures, Her fundoscopic examination, serum and CSF iron level were normal, CBC, liver function tests, serum ceruloplasmin and urinary copper levels were also normal. MRI revealed bilateral symmetrical globus pallidus T1, T2 and FLAIR hypo intensity sparing antero-medial hyper intense foci... features called "eye of the tiger sign"; More manifest on the Diffusion weighted images due to T2 black out effect... features are sequel to focal iron deposition, In view of the patient clinical history the above mentioned features are consistent with Hallervorden-Spatz disease, currently known as Pantothenate kinase-associated neurodegeneration (PKAN)/ Neurodegeneration with brain iron accumulation (NBIA).

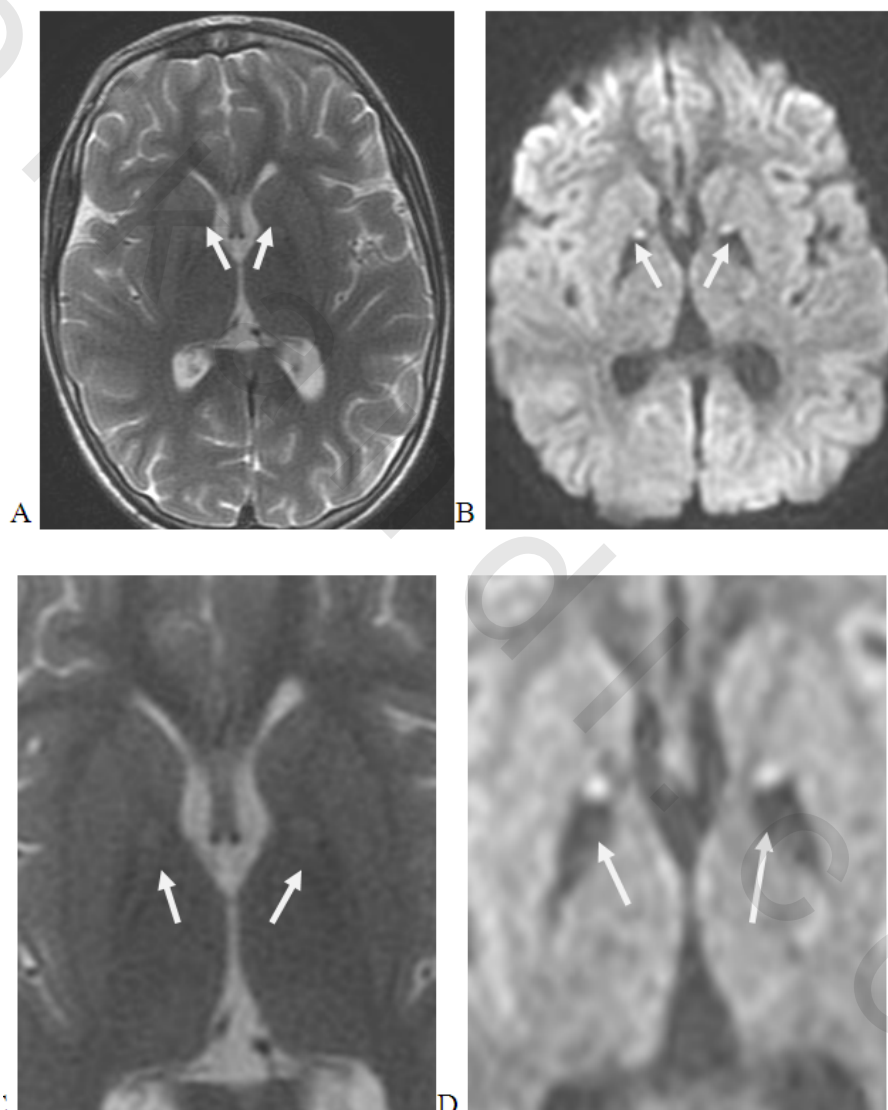


Fig. 35: (A) T2 axial cuts revealed bilateral symmetrical globus pallidus hypointense signals sparing antero-medial hyper intense foci "eye of the tiger sign" (arrow) More manifest on (B) Diffusion weighted images due to T2 black out effect. (C), (D) zoom in of (A), (B) showing the bilateral symmetrical globus pallidus hypointense signals sparing antero-medial hyperintense foci "eye of the tiger sign".

Patient 2: 2 years and half old child presented with psychomotor regression, seizures, dystonia, nystagmus following febrile illness. His weight and height were below the third percentile, but his head circumference was normal. The fundus examination was unremarkable. Laboratory investigation was done it shows elevated lactate pyruvate ratio and CSF examination shows elevated lactate level. MRI revealed T2 and FLAIR hyperintense signal and diffusion restriction within the caudate and lentiform nuclei with involvement of the cerebral peduncle bilaterally and periaqueductal region. MRS analysis from the affected deep gray matter nuclei show mildly decreased NAA/Cr ratio, with preserved Cho/Cr ratio, yet detectable lactate peak (showing inverted doublet) is noted mainly within the globus pallidus bilaterallyfeatures matching with an acute attack of Leigh disease.

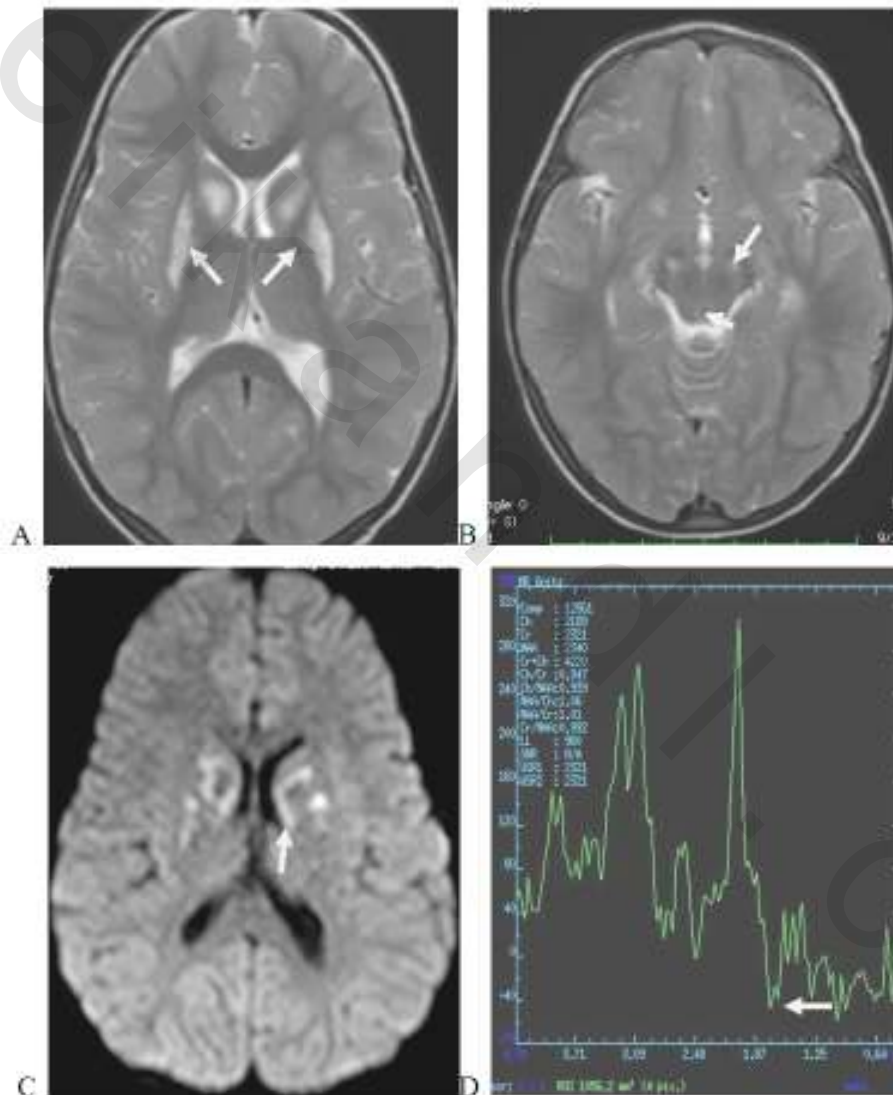


Fig.36: (A) MRI Axial T2 sequence revealed hyperintense signal within the caudate and lentioform nuclei (B) with involvement of the cerebral peduncle and periaqueductal region (arrows) bilaterally. (C) MRI diffusion sequence revealed diffusion restriction within the caudate and lentioform nuclei (D) MRS analysis from the affected deep gray matter, show mildly decreased NAA/Cr ratio, preserved Cho/Cr ratio, detectable lactate peak(inverted doublet)(arrow).

Patient 3: 57 years old male with chronic hepatic failure presented with ascites, ataxia slurred speech and tremors. Lab investigation reveals elevated serum bilirubin, SGOT and SGPT levels. MRI revealed T1 hyperintensity within the globus pallidus nuclei bilaterally, associated with T2 and FLAIR high signal within the sub cortical, periventricular and deep white matter of both cerebral hemispheres, and also associated with T1 hyperintense signal with in the pituitary gland.

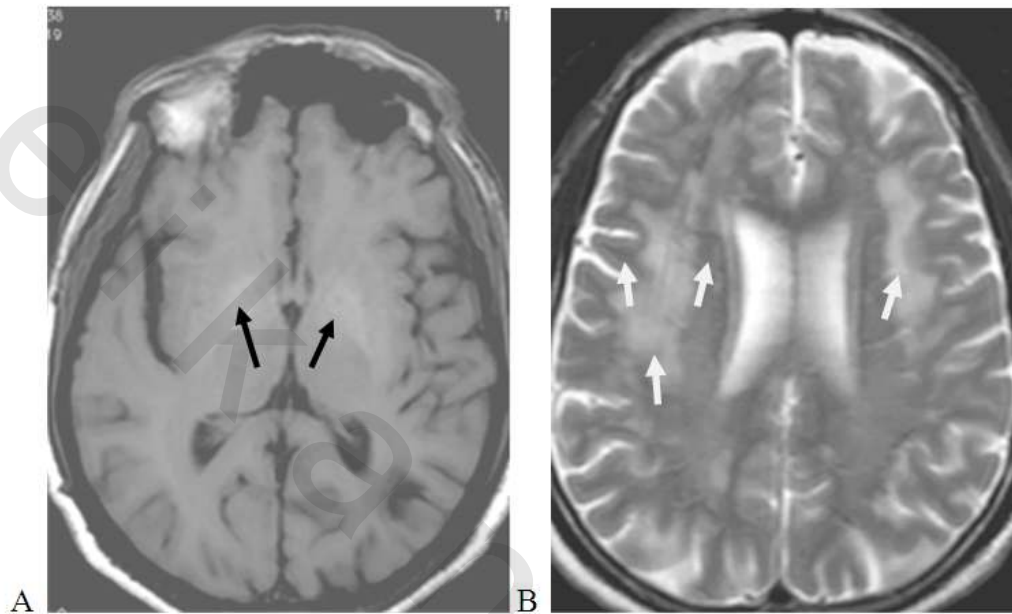


Fig. 37: (A) Axial T1 MRI sequence revealed bilaterally globus pallidus hyperintensity (black arrows). (B) axial T2 MRI sequence reveals high signal intensity within the sub cortical, periventricular and deep white matter (white arrows) of both cerebral hemispheres.

Patient 4: 52 years old male patient with history of HIV infection presented with seizures, ataxia, fever and lymphadenopathy. Laboratory investigations revealed positive anti-toxoplasma Ig G antibodies and Toxo IgM antibodies. MRI revealed bilateral asymmetrical affection of the basal ganglia in the form of T2 and FLAIR hyperintense signal and T1 hypointense signal within the right putamen and the left caudate with post contrast ring and nodular enhancement. The same lesions are noted within the crus cerebri and the gray white matter junction at the fronto-parietal regions and also within the cerebellum ...the final diagnosis was toxoplasmosis.

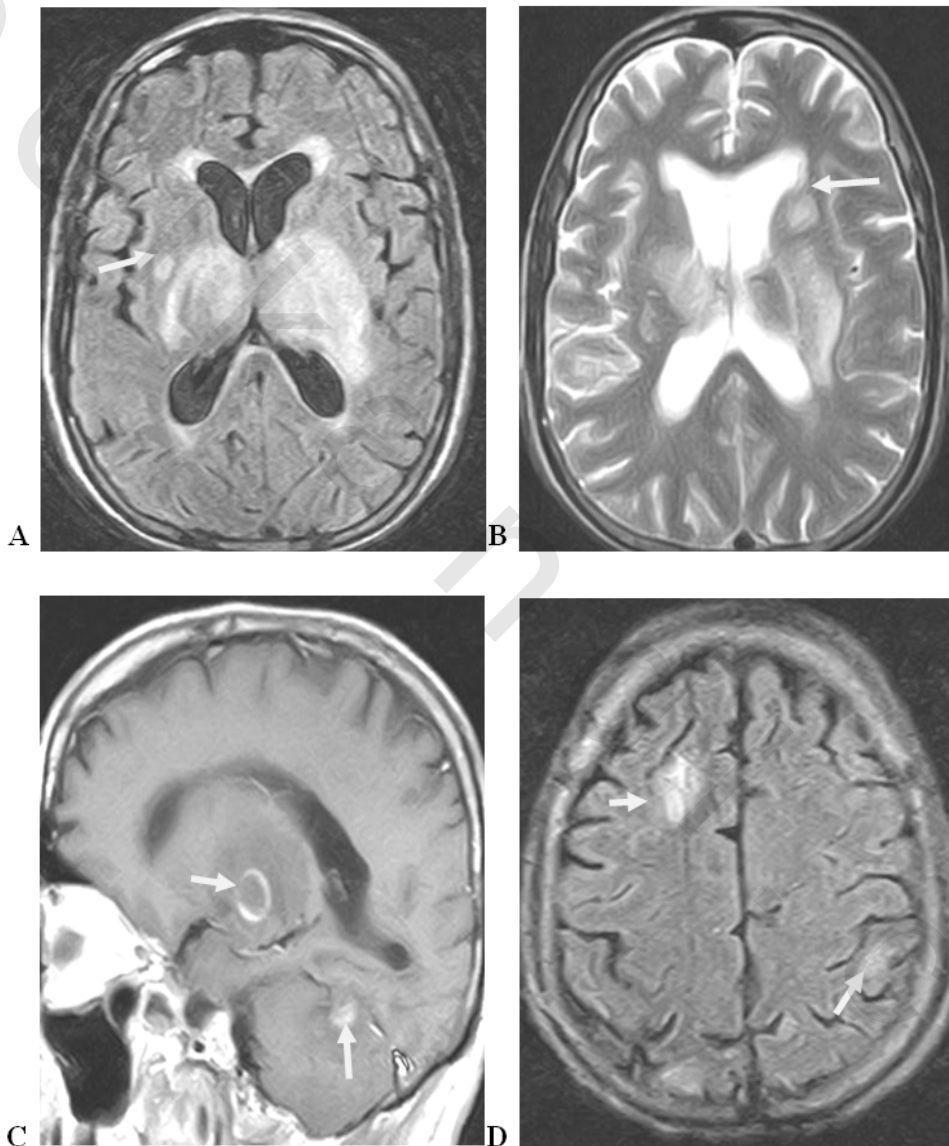


Fig. 38: (A) Axial FLAIR MRI sequence and (B) Axial T2 MRI sequence, revealed bilateral asymmetrical affection of the basal ganglia in the form of T2 and FLAIR hyperintensity within right putamen and left caudate (arrows). (C) Sagittal T1 post contrast MRI sequence revealed post contrast ring and nodular enhancement lesions noted within thalamus and cerebellum respectively (arrows) (D) Axial FLAIR MRI sequence revealed scattered lesions at the gray white matter junction(arrows).

Patient 5: 27 years old male presented with acute loss of consciousness and coma with history of drug abuse, laboratory investigation revealed metabolic acidosis, MRI revealed diffuse gyral swelling, edema in the form of T1 hypointense signal and T2 hyperintense signal involving both cerebral hemispheres symmetrically along the frontal, parietal lobes, both hippocampal regions and the basal ganglia bilaterally (caudate and putamen nuclei) with restricted diffusion... MRI findings are matching with global ischemia.

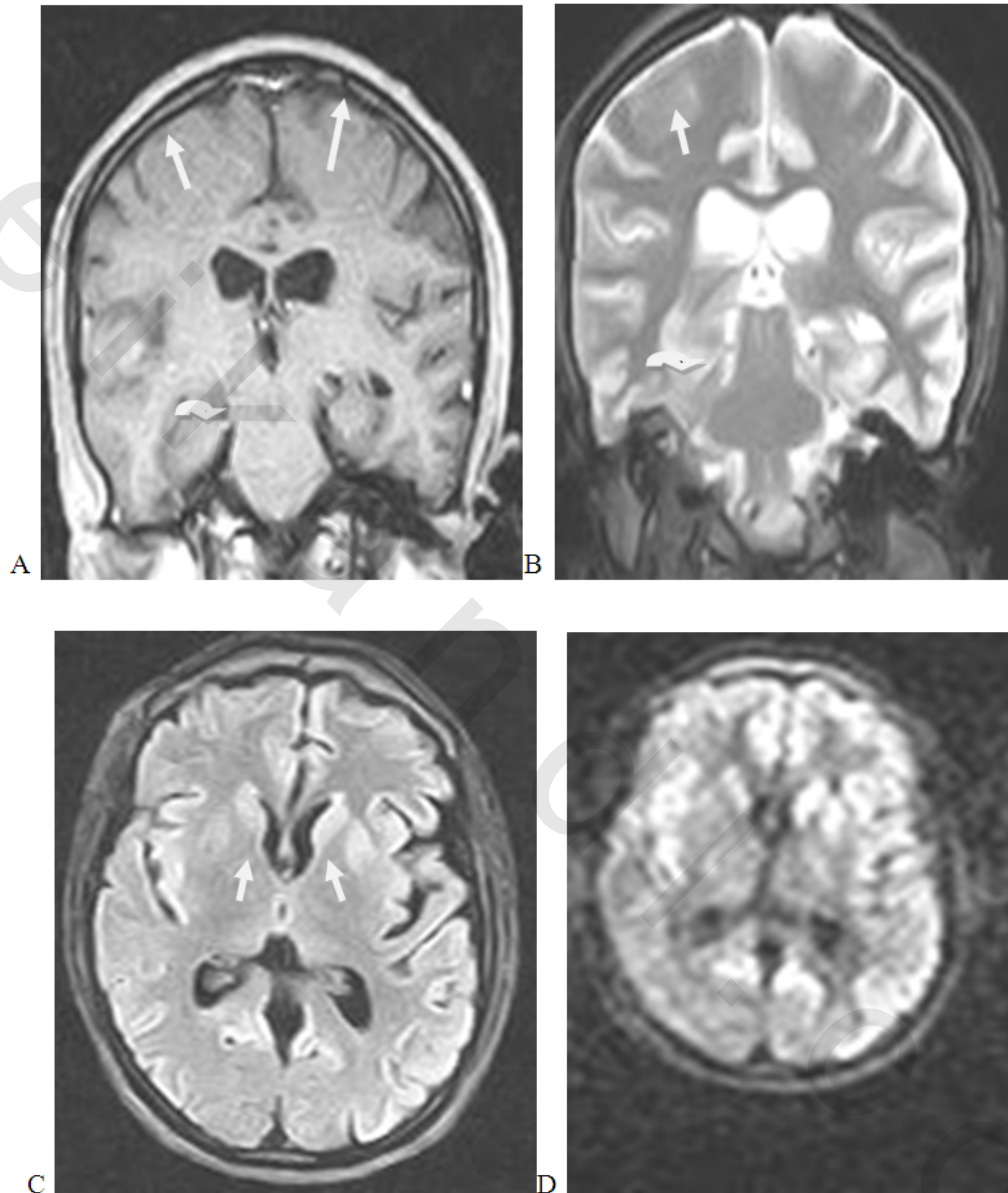


Fig 39: (A) Coronal T1MRI sequence (B) coronal T2 MRI sequence, both revealed diffuse gyral swelling and edema (arrows); T1 hypointense signal and T2 hyperintense signals involving both cerebral hemispheres symmetrically along the frontal, parietal lobes (arrows), both hippocampal regions (curved arrows). (C) Axial FLAIR MRI sequence reveals hyperintense signal of the basal ganglia (caudate and putamen nuclei) (arrows) as well as the hyperintense signal of the swollen gyri. (D) Restricted diffusion of the basal ganglia and the gyri bilaterally.

Patient 6: 13 days old term infant with history of prolonged perinatal asphyxia presented with convulsions and hypotonia. Laboratory investigations revealed metabolic acidosis. MRI revealed T1 hyperintense signal, T2 and FLAIR hypointense signal within the basal ganglia and the ventro-lateral aspect of the thalamus with disappearance of the normal T1 hyperintense signal of the posterior limb of the internal capsule associated with diffuse encephalomalacic changes of both cerebral hemispheres, in the form of T1 hypointense signal and T2 hyperintense signal with restricted diffusion of the basal ganglia, thalamus and periventricular region... features matching with prolonged profound hypoxic ischemic encephalopathy of term neonate.

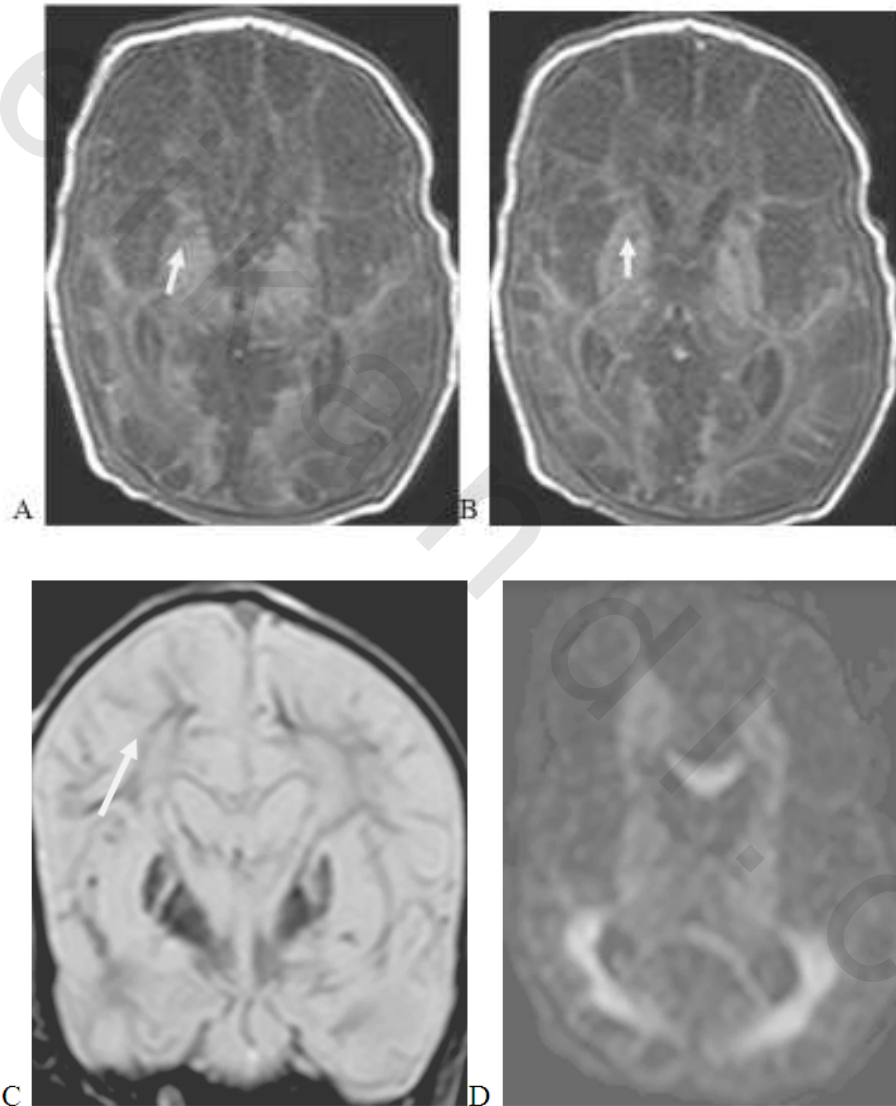


Fig. 40: (A&B) Axial T1 MRI sequence revealed hyperintense signal within the basal ganglia (arrow) and the ventro-lateral aspect of the thalamus, associated with diffuse encephalomalacic changes of both cerebral hemisphere, in the form of T1 hypointense signal. (C) coronal T2 MRI sequence revealed hypointense signal within the basal ganglia associated with hyperintense signals of encephalomalacic changes (arrow). (D) Diffusion MRI sequence shows restricted diffusion of the basal ganglia, thalamus and periventricular region.

patient7: 4 years old male presented with macrocephaly, regression of milestones, motor delay and abnormal movement. MRI revealed bilateral symmetrical affection of the basal ganglia (caudate and putamen nuclei.) In the form of T1 hypointense signal and T2, FLAIR hyperintense signal with atrophic changes and widened ventricles and associated with T2 and FLAIR hyperintense signal of the PVWM and also associated with the characteristic temporal lobe hypoplasia, widened CSF spaces and frontal hygroma sequel of previous extra axial hemorrhage. Laboratory investigation revealed increased urine organic acid/glutaric acid ... MRI features are diagnostic of glutaric acidemia type I.

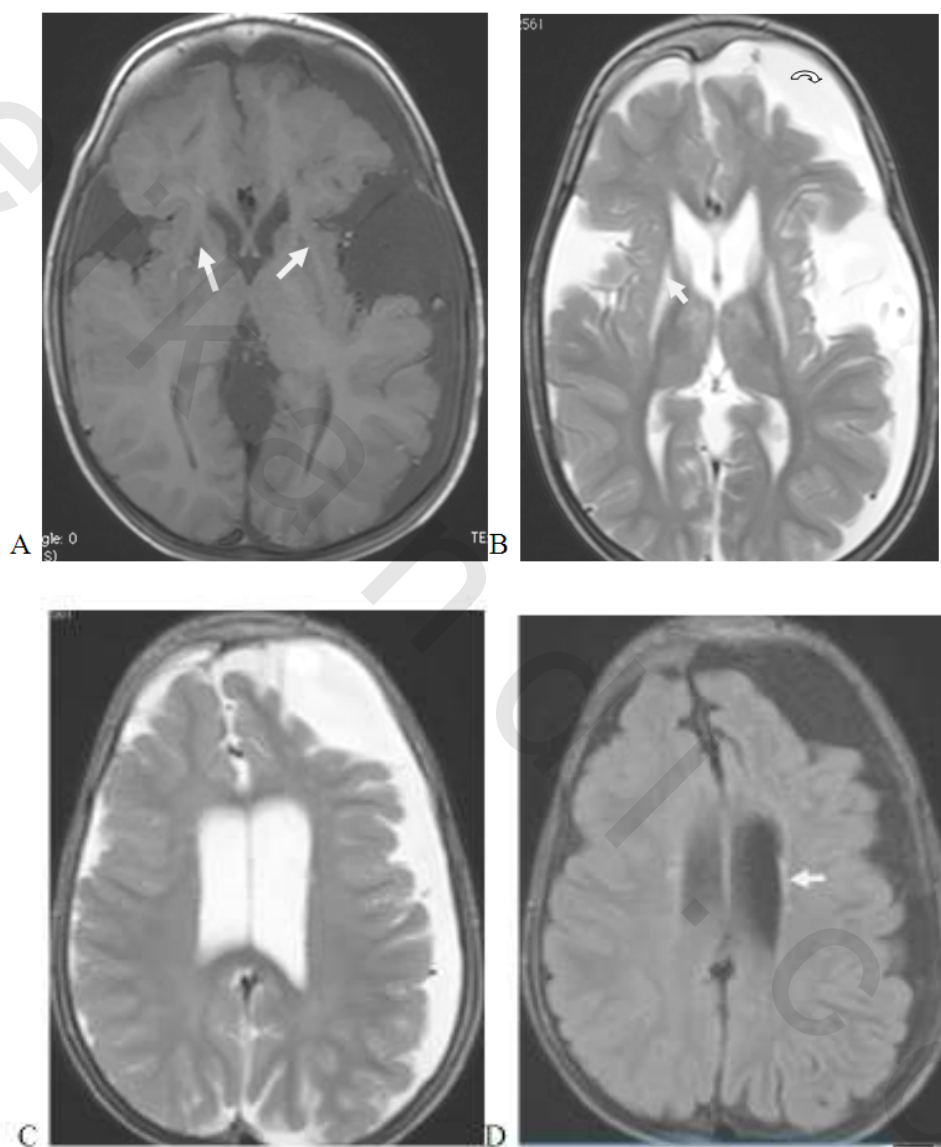
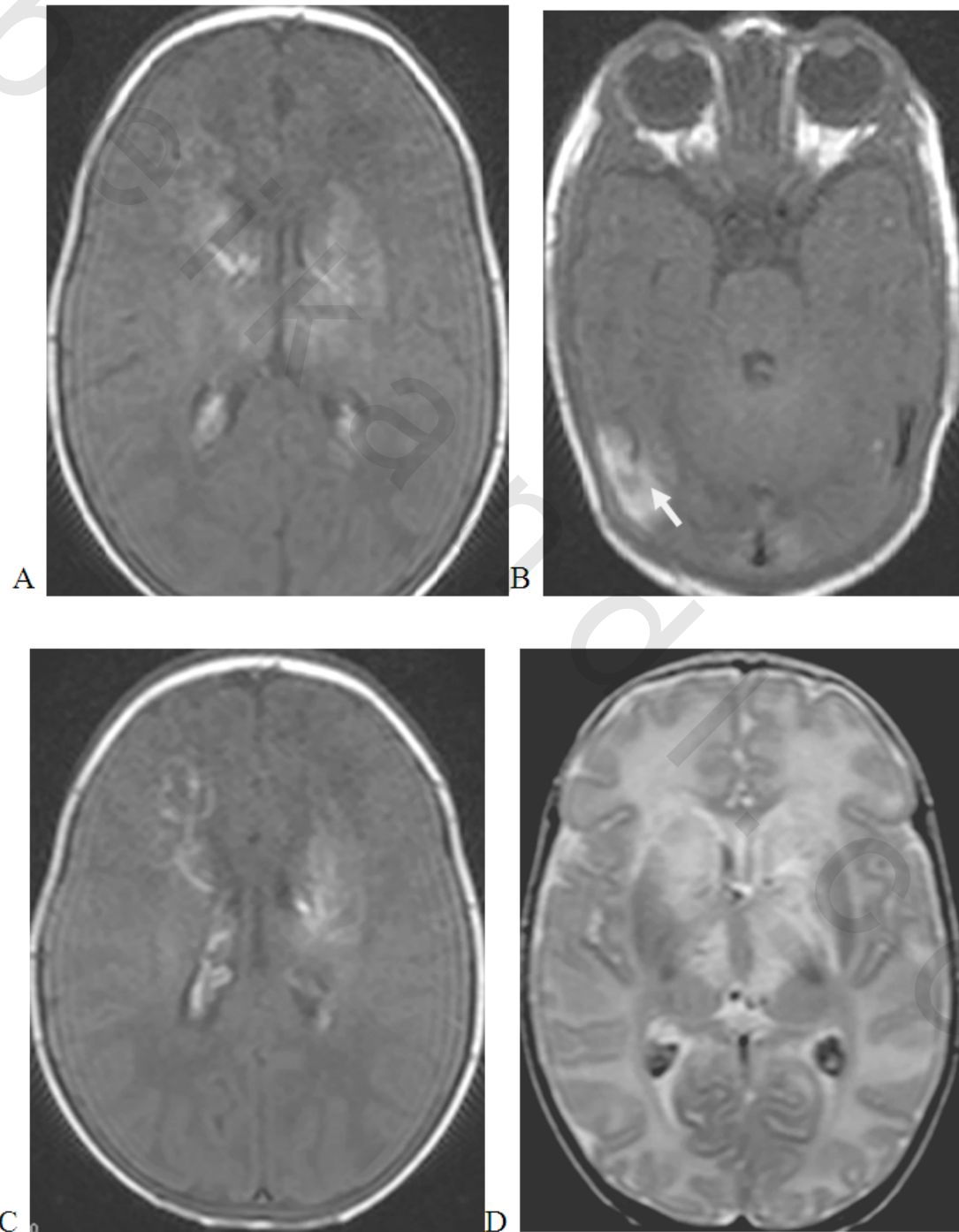


Fig. 41: A) T1 Axial B) - T2 axial. MRI sequences revealed bilateral symmetrical affection of the basal ganglia (caudate and putamen nuclei.) (Arrows) in the form of T1 hypointense and signal T2 hyperintense signal with atrophic changes, widened ventricles and the characteristic temporal lobe hypoplasia, widened CSF spaces and frontal hygroma (curved arrow) C)-Axial T2 D)-Axial FLAIR MRI sequence revealed the widened ventricles and associated with T2 and FLAIR hyperintense signal of the PVWM (arrow).

Patient 8: One month female infant presented with convulsions and abnormal movement. MRI revealed bilateral affection of the basal ganglia and thalamus surrounded by edema in the form of T1 heterogeneous signal mainly hyperintense, T2 and FLAIR hyperintensity with restricted diffusion. T1 revealed hyperintensity along the right transverse sinus reflecting venous sinus thrombosis. MRI venography done and revealed thrombosed right transverse sinus and attenuated internal cerebral veins...MRI features diagnostic of hemorrhagic venous infarction.



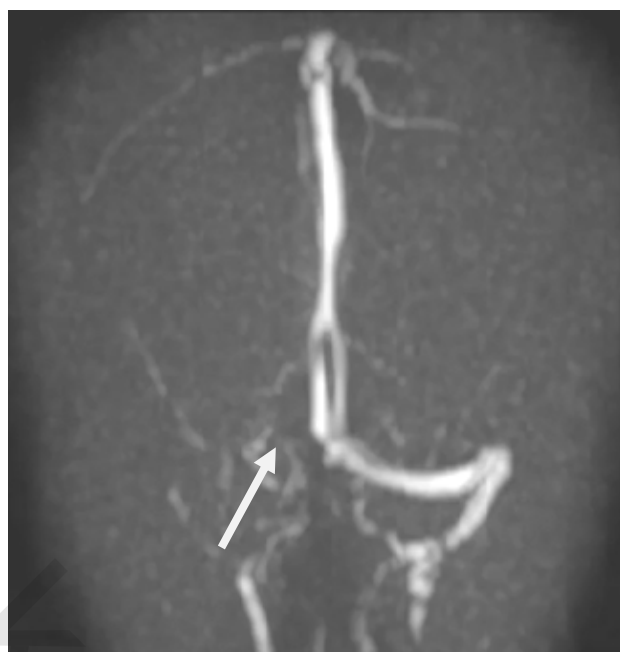


Fig 42: A-B) Axial T1MRI images revealed bilateral affection of the basal ganglia and thalamus surrounded by edema with T1 heterogenous signal B) hyperintensity is noted along the right transverse sinus (arrow) reflecting venous sinus thrombosis. C)axialT1 MRI with hyperintense signal within the lateral ventricle body reflecting hemorrhagic component D)Axial T2 MRI sequence revealed bilateral affection of the basal ganglia and thalamus as bilateral hyperintensities.E)MRI venography revealed non visualization of the right transverse sinus(arrow) ...thrombosed right transverse sinus these was associated with attenuated internal cerebral veins that is not shown.